

# Surface Modification of Tetrafluoroethylene–Hexafluoropropylene (FEP) Copolymer by Remote H<sub>2</sub>, N<sub>2</sub>, O<sub>2</sub>, and Ar Plasmas

Y. W. PARK, S. TASAKA, N. INAGAKI

Laboratory of Polymer Chemistry, Faculty of Engineering, Shizuoka University, 3-5-1 Johoku, Hamamatsu, 432-8561, Japan

Received 2 January 2001; accepted 6 March 2001

**ABSTRACT:** Tetrafluoroethylene–hexafluoropropylene (FEP) copolymer sheets were modified by remote H<sub>2</sub>, N<sub>2</sub>, O<sub>2</sub>, and Ar plasmas, and the effects of the modification on adhesion between FEP sheets and copper metal were investigated. The four plasmas were able to modify the FEP surfaces' hydrophilicity. Defluorination and oxidation reactions on the FEP surfaces occurred with exposure to the plasma. The hydrophilic modification by H<sub>2</sub> plasma was best, followed by modification by O<sub>2</sub>, Ar, and N<sub>2</sub> plasmas. The surface modification of FEP by all four remote plasmas was effective in improving adhesion with copper metal. The peel strength order of the FEP/Cu adhesive joints was H<sub>2</sub> plasma > Ar plasma > N<sub>2</sub> plasma > O<sub>2</sub> plasma. Mild surface modification is important for the adhesion improvement of FEP with Cu metal. © 2002 John Wiley & Sons, Inc. *J Appl Polym Sci* 83: 1258–1267, 2002

**Key words:** tetrafluoroethylene–hexafluoropropylene copolymer; remote plasma; surface modification; adhesion; surface metallization; peel strength; adhesion; fluoropolymers

## INTRODUCTION

Poly(tetrafluoroethylene) (PTFE), is a good polymeric material with high chemical resistance, low surface energy, excellent thermal stability, and high electrical resistivity, but it is not easy to fabricate because of its high crystallinity. Copolymers of tetrafluoroethylene with other fluorinated monomers such as hexafluoropropylene and perfluorovinylether show similar chemical and physical properties to PTFE but also show easy fabrication because of low crystallinity.

Tetrafluoroethylene–hexafluoropropylene (FEP) copolymer is a good electrical insulation material.

The volume resistivity is more than 10<sup>18</sup> Ω cm at 22.8°C, the dielectric constant is 2.1 in a frequency range of 1–10 GHz at 22.8°C, and the dissipation factor is 5 × 10<sup>-4</sup> at 10 MHz and 1.1 × 10<sup>-3</sup> at 1 GHz at 22.8°C.<sup>1</sup> FEP could be expected to be an insulator at extremely high frequencies (in GHz ranges). Printed wiring boards for integrated circuits and an insulator for electric wires are examples of practical applications for FEP. Such applications are composed of FEP and copper metal.

Copper metallization of polymeric materials is possible by many ways, including electroless plating, vacuum deposition, and sputtering of copper metal. Electroless plating is a simple process used to metallize polymer surfaces. In the electroless plating process, reduction reactions of copper ions into copper metal with formaldehyde occur with the assistance of palladium catalysts that are attached on the polymer surface, and a copper

Correspondence to: Y. W. Park (parkyw@mat.eng.shizuoka.ac.jp).

*Journal of Applied Polymer Science*, Vol. 83, 1258–1267 (2002)  
© 2002 John Wiley & Sons, Inc.  
DOI 10.1002/app.2293

metal layer deposits on the surface.<sup>2</sup> This is the essential reaction of copper metallization in the electroless plating process. Therefore, for successful metallization, it is important how one attaches the palladium catalyst on the polymer surface and how one provides strong adhesion between the polymer surface and the deposited copper metal layer. Prior to metallization of FEP, the surface must be modified to become hydrophilic to wet the FEP surface fully with an electroless plating solution and to catch palladium catalysts on the surface. We have reported on a surface-modification technique by remote hydrogen plasma treatment for copper metallization of FEP: The surface modification formed oxygen functional groups such as carboxyl groups (C=O) on the FEP surface. The oxygen functional groups acted as absorption sites for the palladium catalyst.<sup>3</sup>

In this study, instead of hydrogen plasma, other reactive plasmas such as oxygen and nitrogen plasmas were chosen for the surface modification of FEP. We expected that the reactive plasmas would provide hydrophilic properties to the FEP. Xue and colleagues<sup>4,5</sup> proposed that the N—H bond of triazole or imidazole reacts with copper to form an ionic complex. Lee et al.<sup>6</sup> determined that the triazole or imidazole functionality of a polymer forms a complex with copper and that adhesion between the polymer and the copper is enhanced. The N—H group in triazole or imidazole is the active site for the complex (Cu—N) formation. Of course, remote O<sub>2</sub> plasma treatment would make oxygen functional groups that would be expected to combine with hydrogen from exposure to air after treatment. It would also be expected that hydrophilicity can be provided by Ar plasma, which would cut the polymer chains and create end groups.

From the viewpoint of special reactions in the remote plasma, we investigated effects of remote H<sub>2</sub>, N<sub>2</sub>, O<sub>2</sub>, and Ar plasma treatment on the hydrophilicity of FEP surfaces and on the adhesion between the FEP sheet and the copper metal layer.

## EXPERIMENTAL

### Materials

The FEP copolymer sheets were received from Daikin Industries, Ltd. (trade name, Neoflon, Osaka, Japan) in the form of 300 nm wide and 50 μm thick sheets, which were cut to dimensions of 12 × 90 mm and provided as specimens for sur-

face-modification experiments. In this study, we call the copolymer FEP according to custom. Prior to the surface-modification experiment, the FEP sheets were washed with acetone in an ultrasonic washer and dried at room temperature under vacuum. Hydrogen, oxygen, nitrogen, and argon were pure grade, and their purities were 99.9995%.

### Remote H<sub>2</sub>, N<sub>2</sub>, O<sub>2</sub>, and Ar Plasma Treatment of FEP Sheets

A special reactor was used for the remote plasma treatment of the FEP sheets. Details of the reactor were described in a previous article.<sup>7</sup> The reactor consisted of a cylindrical Pyrex glass tube (45 mm in diameter and 1000 mm long) and a columnar stainless steel chamber (300 mm in diameter and 300 mm in height). The Pyrex glass tube had gas inlets for the injection of oxygen, hydrogen, nitrogen, and argon gases and a copper coil of nine turns for the energy input of RF power (frequency = 13.56 MHz). The stainless steel chamber contained a Barocel pressure sensor (type 622, Edwards, UK) and a vacuum system containing a combination of a rotary pump (320 L/min) and a diffusion pump (550 L/sec.; type YH-350 A, Ulvac Co., Tokyo). The Pyrex glass tube was jointed with the chamber in a manner of Vilton O-ring flange.

The FEP sheets were positioned at a constant distance of 800 mm from the center of the copper coil and were exposed to the H<sub>2</sub>, N<sub>2</sub>, O<sub>2</sub>, and Ar plasma separately. First, air in the reaction system was displaced with argon. Afterward, the reaction chamber was evacuated to approximately  $1.3 \times 10^{-2}$  Pa, and then H<sub>2</sub>, N<sub>2</sub>, O<sub>2</sub>, or Ar, whose flow rate was adjusted to 10 cm<sup>3</sup> (STP)/min by a mass flow controller, was introduced into the Pyrex glass tube. The H<sub>2</sub>, N<sub>2</sub>, O<sub>2</sub>, or Ar plasma operated at an RF power of 100 W at 13.56 MHz frequency and at a system pressure of 13.3 Pa for given times (10–180 s).

### Contact Angle of Water

According to the Sessile drop method,<sup>8</sup> contact angles of water on the FEP sheet surfaces treated with the remote H<sub>2</sub>, N<sub>2</sub>, O<sub>2</sub>, and Ar plasma were measured at 20°C with a contact angle meter with a goniometer (model G-1, Erma Co., Ltd., Tokyo). An average contact angle was determined from 10 measurements with an experimental error of 3–4°.

### X-Ray Photoelectron Spectra

X-ray photoelectron spectroscopy (XPS) spectra for FEP surfaces treated with remote plasma were obtained on a Shimadzu ESCA K1 (Tokyo) spectrometer with a nonmonochromatic MgK $\alpha$  photon source at an anode voltage of 12 kV, an anode current of 20 mA, and a pressure in the analytical chamber of  $1.5 \times 10^{-6}$  Pa. The XPS spectra were referenced with respect to 690.0 eV fluorine 1s core level to eliminate charging effects. The spectra were not modified by the smoothing procedure. We decomposed the C<sub>1s</sub> and O<sub>1s</sub> spectra by fitting a Gaussian–Lorentzian mixture function (mixture ratio = 80:20) to an experimental curve with a nonlinear, least squares curve-fitting program (ESCAPAC) supplied by Shimadzu. Sensitivity factors (S) for the C<sub>1s</sub>, O<sub>1s</sub>, F<sub>1s</sub>, and Cu<sub>2p3/2</sub> core levels were as follows: S(C<sub>1s</sub>) = 1.00, S(O<sub>1s</sub>) = 2.85, S(F<sub>1s</sub>) = 4.26, and S(Cu<sub>2p3/2</sub>) = 15.87. The F/C and O/C atomic ratios were calculated from the F<sub>1s</sub>, O<sub>1s</sub>, and C<sub>1s</sub> intensities, and their experimental error was within 0.03.

### Copper Metallization of FEP Surfaces

FEP surfaces were metallized by electroless plating, and then the copper layer deposited on the FEP surfaces was thickened by electroplating. The total thickness of the deposited copper metal was about 30  $\mu\text{m}$  (0.2  $\mu\text{m}$  thickness by the electroless plating and 30  $\mu\text{m}$  thickness by the electroplating). In the electroless plating process, first the FEP sheets, whose surfaces were modified to become hydrophilic by the remote H<sub>2</sub>, N<sub>2</sub>, O<sub>2</sub>, and Ar plasma treatment, were placed in a special solution (a mixture of OPC-80 and OPC-SAL, Okuno Chemical Industries Co., Ltd., Osaka, Japan) containing colloidal palladium–tin alloy particles, which acted as a catalyst for reduction reactions from copper ions to copper metal, and were kept in the solution at 25°C for 5 min to attach the colloidal palladium–tin alloy particles on the FEP surfaces. Then, the FEP sheets were treated with dilute sulfuric acid solution (3.6M) at 40°C for 5 min to make the surfaces of the colloidal particles palladium-rich by dissolution of the tin component alone in the sulfuric acid solution. Afterward, the FEP sheets were put in a special electroless plating solution (TMP; Okuno Chemical Industries) at room temperature for 5 min to deposit copper metal on the FEP surfaces.

Surfaces of the FEP sheets were made electrically conductive by the electroless plating procedure, which was carried out at a constant current

of 10 A (current density = 300 A/m<sup>2</sup>) and at a constant voltage of 8 V at 24°C for 1 h in a sulfuric acid solution (190 g/L) containing copper sulfate (75 g/L), hydrogen chloride (50 ppm), and a glossy reagent (5 mL of PCM, Nippon Rironal Co., Osaka, Japan). Finally, the FEP sheets were washed with water and dried at 80°C for 12 h under vacuum.

### Peel Strength of the Adhesive Joint Between the FEP Sheet and Copper Metal

The T-type peel strength (5 mm wide) of the adhesive joint between the FEP sheets and copper metal was evaluated at a peel rate of 10 mm/min with an Instron-type tensile strength tester (Shimadzu AGS 100-A). The peel strength was determined from an average of 10 measurements.

### Atomic Force Microscopy (AFM)

The topographic measurements of untreated FEP sheets and remote plasma-treated FEP sheets were done on a Seiko (Tokyo) instrument SPI3700 to observe their surface configurations. A triangular–pyramidal silicon nitride tip was used as a probe, and an area of  $2 \times 2 \mu\text{m}$  was scanned under a probe pressure of  $8.7 \times 10^{-11}$  N/m<sup>2</sup>. An arithmetic mean of the surface roughness ( $R_a$ ) was calculated from the roughness profile determined by AFM.

## RESULTS AND DISCUSSION

### Chemical Composition of the FEP Sheets Modified by Remote H<sub>2</sub>, O<sub>2</sub>, N<sub>2</sub>, and Ar Plasmas

The FEP surfaces were exposed to the H<sub>2</sub>, O<sub>2</sub>, N<sub>2</sub>, and Ar plasmas to assess effects of the plasmas on the surface modification. Figure 1 shows the typical contact angles of water against the FEP surfaces treated with the plasmas at 100 W as a function of the plasma treatment time. The contact angles, as shown in Figure 1, decreased considerably within a short time of 10 s as soon as the FEP surfaces were exposed to the plasmas, and the decrease continued up to 40 s. The contact angle reached equilibrium at a plasma treatment time of about 50 s, after which the contact angle was constant. The contact angle at equilibrium depended strongly on which plasma was used for the surface modification. The contact angles at 60 s were 77, 92, 104, and 104° in the H<sub>2</sub>, O<sub>2</sub>, N<sub>2</sub>, and Ar plasma treatments, respectively. This indicates that which plasma was used for the modification rather than how long the FEP surfaces

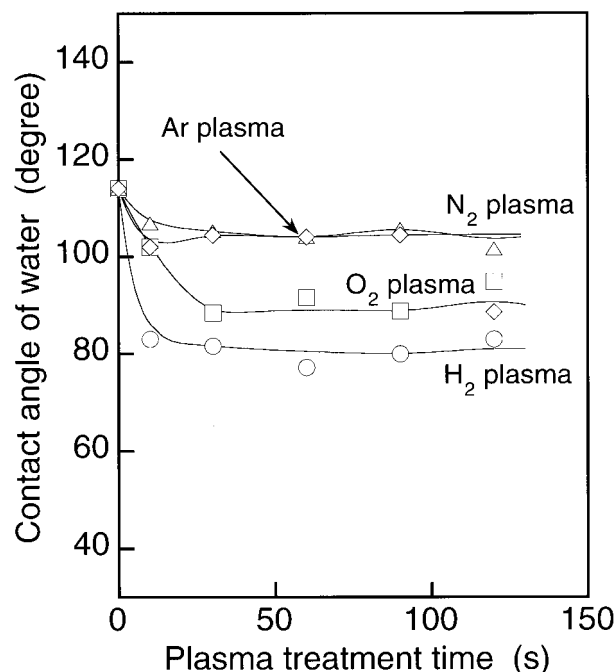


**Figure 1** Contact angle of water on the FEP with remote plasma treatments as a function of the exposure time (RF power = 100 W).

were exposed to the plasma was the important factor in the surface modification of FEP. From the viewpoint of the contact angle, the hydrogen plasma was the most effective for the modification, and the nitrogen and argon plasmas were not so effective. The oxygen plasma was not as effective as expected.

Atom composition for the plasma-treated FEP surfaces was calculated from the relative intensity of the  $C_{1s}$ ,  $F_{1s}$ ,  $O_{1s}$ , and  $N_{1s}$  spectra. Table I shows F/C, O/C, and N/C atom ratios for the FEP surfaces treated with the  $H_2$ ,  $O_2$ ,  $N_2$ , and Ar plasmas at 100 W for 60 s. The F/C atom ratio for the

untreated FEP was 1.9, which was slightly lower than that calculated from the repeating unit ( $F/C = 2.0$ ), and the O/C atom ratio was less than 0.03. All plasma-treated FEP surfaces, as shown in Table I, showed a lower F/C ratio (0.80–1.6) and higher O/C ratio (0.08–0.14) than the untreated FEP surface. These changes in atom composition indicate that defluorination and oxidation reactions occurred on the FEP surfaces with all plasmas. Furthermore, in the remote  $N_2$  plasma treatment, a very low N/C atom ratio (0.03) was observed, indicating that some nitrogenation occurred in the FEP surface. From these results, we can conclude that main modifications occurring on the FEP surfaces by the plasmas were due to defluorination and oxidation. Reactivity of the defluorination and oxidation, as shown in Table I, strongly depended on which plasma was used for the modification of the FEP surface. The oxygen plasma showed the highest reactivity for defluorination ( $F/C$  atom ratio = 0.80). A F/C atom ratio of 0.80 corresponded to 58% of fluorine atoms on the FEP surface being removed. On the other hand, hydrogen plasma showed the lowest reactivity ( $F/C$  atom ratio = 1.6). Hydrogen plasma removed only 16% of the fluorine atoms from the FEP surface. The nitrogen and argon plasmas showed a medium reactivity of the four plasmas. Forty-three percent of fluorine atoms were removed from the FEP surfaces by the nitrogen and argon plasmas. With regard to oxidation, hydrogen and oxygen plasmas showed higher reactivities than nitrogen and argon plasmas. A combination of the contact angle (Fig. 1) and atom composition (Table I) for the plasma-treated FEP surfaces points out that the degree of defluorination initiated by the plasma did not always show a relationship with the decreased contact angle on the plasma-treated FEP surfaces. Defluorination

**Table I** Chemical Composition of Remote  $H_2$ ,  $N_2$ ,  $O_2$ , and Ar Plasma-Treated FEP Surfaces

Plasma Treatment Conditions			Atomic Ratio			Relative Concentration of $C_{1s}$ Components (%)				
						$\text{CH}-\text{CF}_n$ and $\text{C}-\text{O}$	$\text{CHF}-\text{CF}_n$ and $\text{O}-\text{CF}-\text{CF}_n$	$\text{O}=\text{C}-\text{CF}_n$ and $\text{O}-\text{CHF}-\text{CF}_n$	$\text{CF}_2$	$\text{CF}_3$
Gas	RF Power (W)	Treatment Time (s)	F/C	O/C	N/C					
—	—	—	1.9	< 0.03					96	4
$O_2$	100	60	0.8	0.13		28	9	6	51	6
$N_2$	100	60	1.1	0.08	0.03	14	6	5	69	6
Ar	100	60	1.1	0.10		5	3	4	65	23
$H_2$	100	60	1.6	0.14		4	8	14	71	3

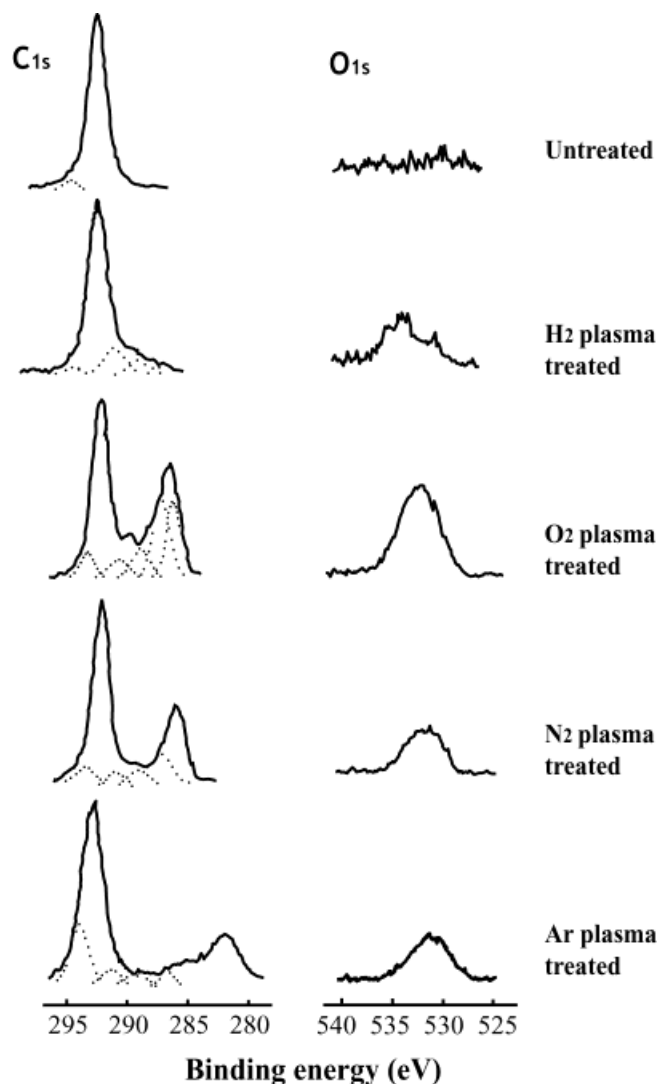
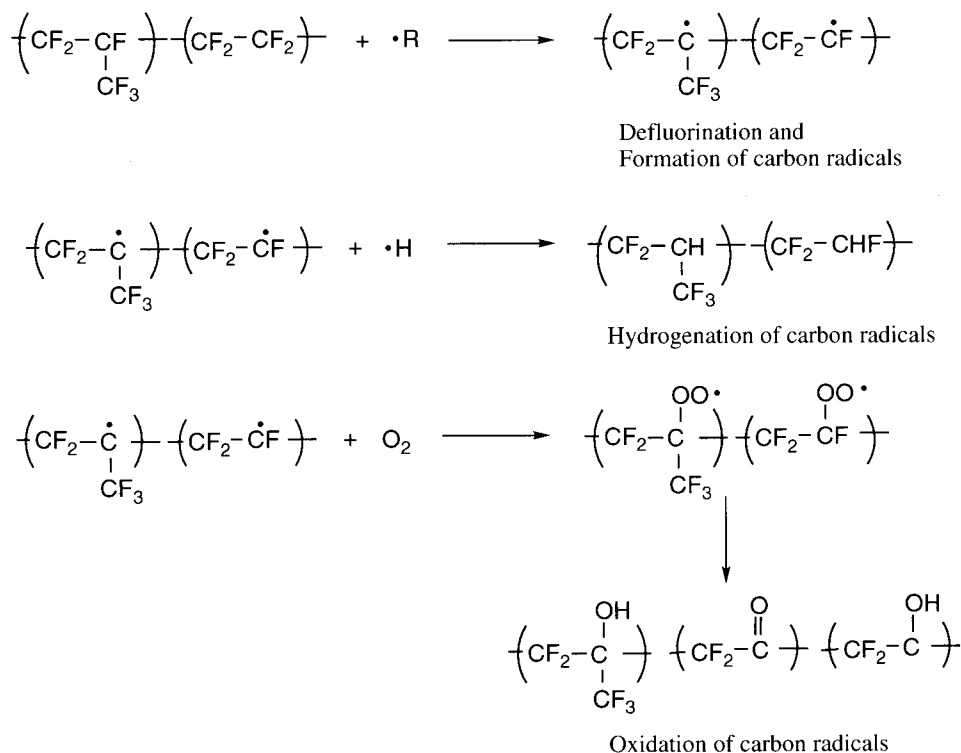


**Figure 2** XPS ( $C_{1s}$ ,  $O_{1s}$ ) spectra for FEP surfaces untreated and treated with the remote  $H_2$ ,  $O_2$ ,  $N_2$ , and Ar plasmas at 100 W for 60 s.

by the oxygen plasma was 58%, and contact angle was  $92^\circ$ , but on the other hand, hydrogen plasma showed a reactivity of 16%, and the contact angle on the plasma-treated FEP surface was  $77^\circ$ .

The chemical composition of the plasma-treated FEP surfaces was analyzed by XPS spectra, mainly  $C_{1s}$  spectra. Figure 2 shows typical  $C_{1s}$  and  $O_{1s}$  spectra for the FEP surfaces treated with the four plasmas at 100 W for 60 s.  $F_{1s}$  spectra were eliminated from the figure because the spectra did not change and had a monotone distribution even after the plasma treatment. Although the  $N_2$  plasma-treated FEP surfaces showed  $N_{1s}$  spectra, the spectra are not shown here because the quality (S/N ratio) of the spectra was poor due to a low concentration of nitrogen

atoms on the plasma-treated FEP surfaces. The  $C_{1s}$  spectra, as shown in Figure 2, were decomposed into five components, which are illustrated as dotted lines in the spectra. The five components were positioned at 286.9, 288.9, 291.1, 292.5, and 294.6 eV, which were assigned to  $\underline{C}H-CF_n$  and  $\underline{C}-O$ ;  $\underline{C}HF-CF$ ,  $O-\underline{C}F-CF_n$ , and  $\underline{C}(O)-CF$ ;  $O=\underline{C}-CF_n$ , and  $O-\underline{C}HF-CF$ ;  $\underline{C}F_2$ ; and  $\underline{C}F_3$  groups, respectively. Underlining indicates the assigned carbons. The relative concentrations of these components were estimated from the relative peak areas, and the results of the estimation are listed in Table I. Table I shows that the plasma treatments caused the defluorination of  $CF_2$  groups to form new defluorinated carbon components, such as CH, CHF, C—O, and



Scheme 1

C=O groups. In addition to these components, the CF<sub>3</sub> component also was formed by the plasma treatments.

Generally, plasma treatment gives two essentially different processes to modify surface properties in chemical and physical meanings. The essential processes are the introduction of functional groups such as carbonyl, carboxyl, and hydroxyl groups onto polymer surfaces and the etching of the polymer surface layer (degradation reactions) to modify the surface morphology. We believe that the former process could proceed from radical reactions between radicals in plasma and polymer surface. On the other hand, the latter process could proceed from the bombardment of electrons and ions in plasma on polymer surfaces. The defluorinated carbon components such as CH, CHF, C—O and C=O groups may be the result of combination reactions with defluorination and oxidation. Radicals in the plasmas would remove fluorine atoms from FEP surfaces to form carbon radicals in the FEP polymer chains. Some of the carbon radicals would combine with radicals such as hydrogen, oxygen, and nitrogen in plasmas to form functional components such as C—H, C—O, and C—N groups on the FEP surface. Other carbon radicals on the FEP surfaces would remain even after the plasma treatment,

and the carbon radicals, when the FEP surfaces were taken out from the plasma reactor, would be oxidized by air to form oxygen components such as C=O groups. These reactions are shown in Scheme 1 for the hydrogen plasma treatment.

On the other hand, the etching process degrades the FEP surfaces. Electrons and ions with high kinetic energy in the plasmas would collide with FEP surfaces. As a result, the C—C bond scission would occur to form radicals at the end of polymer chains and would initiate degradation reactions from the polymer chain end. Therefore, we believe that the CF<sub>3</sub> component may be the result of C—C bond scission in FEP polymer chains. From this viewpoint, we discuss what is different in the surface modification by the four plasmas. The formation of  $\underline{\text{C}}\text{H}-\text{CF}_n$  and  $\underline{\text{C}}-\text{O}$ ;  $\underline{\text{C}}\text{HF}-\text{CF}$ ,  $\text{O}-\underline{\text{C}}\text{F}-\text{CF}_n$ , and  $\underline{\text{C}}(\text{O})-\text{CF}$ ;  $\text{O}=\underline{\text{C}}-\text{CF}_n$ , and  $\text{O}-\underline{\text{C}}\text{HF}-\text{CF}$  groups was due to the combination reactions of defluorination and oxidation by radicals. The formation of the  $\underline{\text{C}}\text{F}_3$  group was due to the etching reactions by the electron and ion collision.

Table I distinguishes the features of surface modification by the plasmas. In the hydrogen plasma treatment, the extent of the defluorination was low (29%), but the relative concentration of  $\text{O}-\underline{\text{C}}\text{F}-\text{CF}_n$  and  $\underline{\text{C}}(\text{O})-\text{CF}$  groups was high

**Table II Surface Roughness of Remote Plasma-Treated FEP Film at 100 W for 60 s**

	Gas				
	—	O <sub>2</sub>	H <sub>2</sub>	N <sub>2</sub>	Ar
Surface Roughness ( <i>R<sub>a</sub></i> ) (nm)	4.10	3.99	4.78	3.85	2.78

(14%) and the concentration of the CF<sub>3</sub> group was small (3%). In the oxygen and nitrogen plasma treatments, the extent of the defluorination was high (49%), and the relative concentration of  $\underline{\text{C}}\text{H}-\text{CF}_n$  and  $\underline{\text{C}}-\text{O}$  groups was high (28%), and also the concentration of the CF<sub>3</sub> group was small (6%). The nitrogen plasma treatment also showed a high relative concentration of  $\underline{\text{C}}\text{H}-\text{CF}_n$  and  $\underline{\text{C}}-\text{O}$  groups (14%), and a low concentration of the CF<sub>3</sub> group (6%). In the argon plasma treatment, the relative concentration of  $\underline{\text{C}}\text{F}_3$  groups was very high (23%), and the concentration of other components, such as  $\underline{\text{C}}\text{H}-\text{CF}_n$  and  $\underline{\text{C}}-\text{O}$ ;  $\underline{\text{C}}\text{H}\text{F}-\text{CF}$ ,  $\text{O}-\underline{\text{C}}\text{F}-\text{CF}_n$ , and  $\underline{\text{C}}(\text{O})-\text{CF}$ ;  $\text{O}=\underline{\text{C}}-\text{CF}_n$ , and  $\text{O}-\underline{\text{C}}\text{H}\text{F}-\text{CF}$  groups were 3–5%. This comparison indicates that the surface modification by hydrogen, oxygen, and nitrogen plasmas is essentially different from that by argon plasma. The hydrogen, oxygen, and nitrogen plasmas caused surface modification by radical reactions in the plasmas that initiated introduction reactions of oxygen and nitrogen functional groups on the FEP surfaces, whereas the argon plasma caused surface modification by electron and ion collisions that initiated degradation reactions on the FEP surfaces. This prediction could be confirmed from changes in the surface roughness.

Table II shows the surface roughness of the FEP surfaces as a function of plasma. The surface roughness (*R<sub>a</sub>*) was estimated from 2 × 2 μm AFM pictures. The argon plasma treatment, as shown in Table II, led to a large change in the surface roughness from 4.10 to 2.78 μm (−1.36 μm). On the other hand, the hydrogen, oxygen, and nitrogen plasmas never showed a large change. The roughness change was as small as −0.25 to 0.68 μm (from 4.10 to 4.78–3.85 μm). This large change indicates that in the argon plasma, the etching process rather than the introduction process of functional groups may have been predominant. For hydrogen, oxygen, and nitrogen plasmas, the introduction process of functional groups rather than the etching process may have been predominant.

We can then summarize features of the hydrogen, oxygen, nitrogen, and argon plasmas. The hydrogen plasma led to low reactivity in defluorination and high reactivity in oxidation. The oxygen plasma led to high reactivity in defluorination and oxidation. The nitrogen plasma led to high reactivity in defluorination. For three plasmas, the etching process was negligible. On the other hand, argon plasma led to high etching process and high defluorination.

### Copper Metallization of FEP Surfaces by a Combination of Electroless Plating and Electroplating

The results from XPS spectra show essential differences in the modification reactions of the FEP surfaces by hydrogen, oxygen, nitrogen, and argon plasmas. Differences in how these modification reactions by the four plasmas influenced adhesion between copper metal and FEP was investigated. The FEP sheets were treated with H<sub>2</sub>, N<sub>2</sub>, O<sub>2</sub>, and Ar plasmas at 100 W for 60s, and then, on the plasma-treated FEP surfaces, a copper metal layer (30 μm thick) was deposited by a combination of electroless plating and electroplating. Table III shows the peel strength for copper metal/FEP adhesive joints as a function of plasma. The untreated FEP showed no adhesion with the copper metal layer. Table III shows that surface modification by the H<sub>2</sub>, N<sub>2</sub>, O<sub>2</sub>, and Ar plasmas led to great improvement in peel strength and that the kind of plasma used for the surface modification strongly influenced the peel strength. Hydrogen plasma gave the highest peel strength (199 mN/5mm), and argon and nitrogen plasmas followed. The peel strength was 71 and 56 mN/5mm for argon and nitrogen plasmas, respectively. Oxygen plasma was not effective for the improvement of adhesion. Its peel strength was 27 mN/5mm.

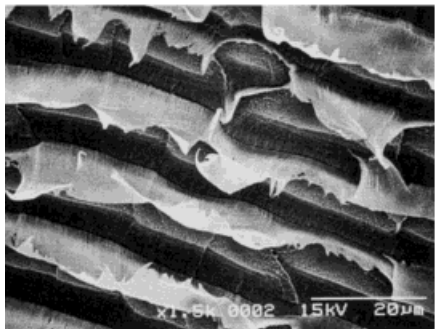
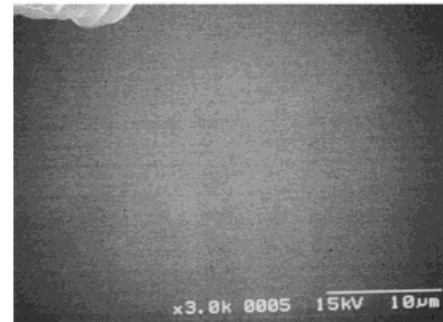
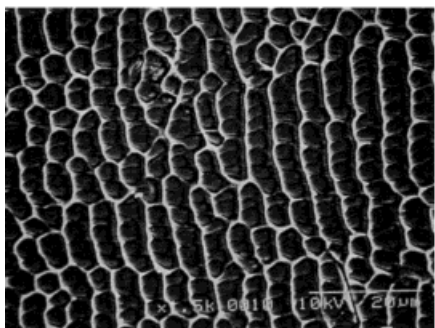
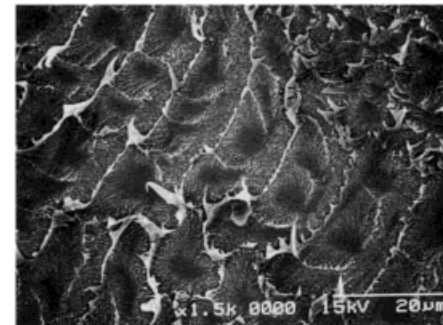
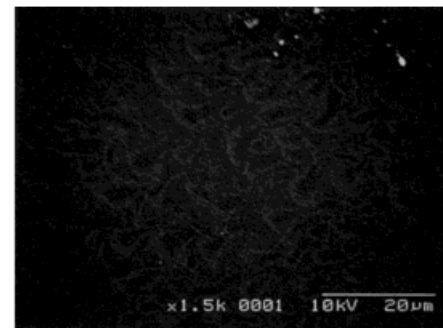
To investigate where the copper/FEP adhesive joints were failing in the peel strength measure-

**Table III Peel Strength of Plasma-Treated FEP/Copper Metal Adhesive Joints**

Plasma	RF Power (W)	Treatment Time (s)	Peel Strength (mN/5 mm)
H <sub>2</sub>	100	60	199
O <sub>2</sub>	100	60	27
N <sub>2</sub>	100	60	56
Ar	100	60	71
Untreated			0

## FEP polymer side

## Cu metal side

Cu/Untreated  
FEP systemCu/remote H<sub>2</sub>  
plasma treated  
FEP systemCu/remote O<sub>2</sub>  
plasma treated  
FEP system

**Figure 3** SEM pictures of the FEP polymer and Cu metal layers peeled off from the Cu/FEP system.

ment, the surfaces of peeled-off layers (copper and FEP layers) were observed with scanning electron microscopy (SEM) and XPS. For the observations,

three adhesive joints, the copper/untreated FEP, the copper/hydrogen plasma-treated FEP, and the copper/oxygen plasma-treated FEP adhesive



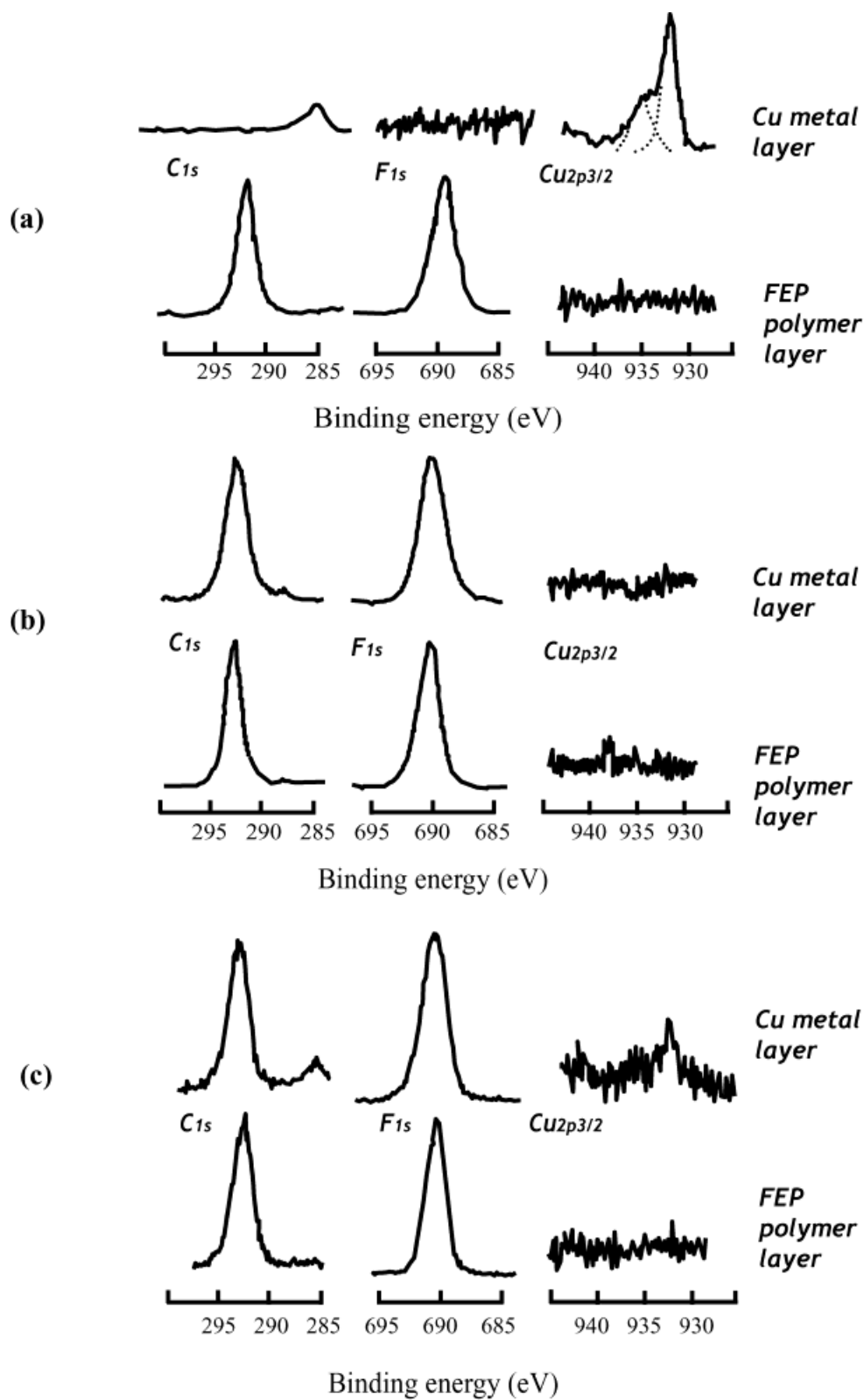


**Figure 4** Figure 4: XPS ( $C_{1s}$ ,  $F_{1s}$ ,  $Cu_{2p3/2}$ ) spectra for the FEP polymer and Cu metal layers peeled off from the (a) Cu metal/untreated FEP system, (b) Cu metal/remote H<sub>2</sub> plasma-treated FEP system, and (c) Cu metal/remote O<sub>2</sub> plasma-treated FEP system.

joints, were used. Figure 3 shows typical SEM pictures of the peeled-off two layers. For the copper/untreated FEP adhesive joint, the two peeled-off layers, as shown in Figure 3, were smooth. On the other hand, for the copper/hydrogen plasma-treated FEP and the copper/oxygen plasma-treated FEP adhesive joints, the layers showed complex surfaces with thin and stretched pieces. The layers peeled-off from the copper/hydrogen plasma-treated FEP adhesive joint showed an especially heavy locus of failure. The XPS analyses answered the question regarding the locus of failure. The same layer surfaces used for the SEM observation were used as specimens for XPS analyses. Figure 4(a,b,c) shows  $C_{1s}$ ,  $F_{1s}$ , and  $Cu_{2p3/2}$  spectra for two layers peeled-off from the copper/untreated FEP, the copper/hydrogen plasma-treated FEP, and copper/oxygen plasma-treated FEP adhesive joints. As shown in Figure 4(a), the two layers showed completely different  $C_{1s}$ ,  $F_{1s}$ , and  $Cu_{2p3/2}$  spectra. As shown in Figure 4(b), the two layers peeled-off from the copper/hydrogen plasma-treated FEP adhesive joint showed similar XPS spectra. The  $C_{1s}$  spectra resembled that of the original FEP (Fig. 2). As shown in Figure 4(c), the layers resembled the layers from the copper/hydrogen plasma-treated FEP adhesive joints, but they were different in some points. From these results, we believe that the failure mode of the copper/plasma-treated FEP adhesive joints was as follows.

In the copper/untreated FEP adhesive joint, failure occurred mainly at the interface between the copper and FEP layers. In the copper/hydrogen plasma-treated FEP adhesive joint, failure occurred at an inner FEP layer near the interface. In the copper/oxygen plasma-treated FEP adhesive joint, failure occurred at the plasma-modified FEP layer near the interface.

## CONCLUSIONS

FEP sheets were modified with remote  $H_2$ ,  $N_2$ ,  $O_2$ , Ar plasmas, and the effects of modification on the adhesion between the copper layer and FEP sheet

were investigated. Use of remote  $H_2$ ,  $N_2$ ,  $O_2$ , and Ar plasmas is preferable for the surface modification of the copper metal/FEP system. Our results are summarized as follows:

1. Remote  $H_2$ ,  $N_2$ ,  $O_2$ , and Ar plasma treatment for a short time of 10 s was able to make the FEP surface relatively hydrophilic. Hydrophilic modification by  $H_2$  plasma was best, followed by modification by  $O_2$ , Ar, and  $N_2$  plasmas.
2. Remote  $H_2$ ,  $N_2$ ,  $O_2$ , and Ar plasma treatment caused defluorination and oxidation of the FEP surface.
3. The modification of the FEP surface by the remote  $H_2$ ,  $N_2$ ,  $O_2$ , and Ar plasmas were effective for the adhesion to copper metal. The peel strength order for the FEP/Cu adhesive joints was  $H_2 > Ar > N_2 > O_2$  plasma. Mild surface modification was good for the adhesion improvement of FEP with Cu metal.

## REFERENCES

1. Encyclopedia of Polymer Science and Technology; Bikales, N. M., Ed.; Interscience: New York, 1971; Vol. 13, p 623.
2. Okuno, K. Hyomen Gijutsu (in Japanese) 1993, 44, 578.
3. Inagaki, N.; Tasaka, S.; Park, Y. W. J Adhes Sci Technol 1998, 12, 1105.
4. Xue, G.; Dau, Q.; Jiang, S. J Am Chem Soc 1988, 10, 2393.
5. Xue, G.; Dong, J.; Zhang, J. Macromolecules 1991, 24, 4185.
6. Lee, K.-W.; Walker, G. F.; Viehbeck, A. J Adhes Sci Technol 1995, 9, 1125.
7. Yamanda, Y.; Yamanda, T.; Tasaka, S.; Inagaki, N. Macromolecules 1996, 29, 4331.
8. Garbassi, F.; Morra, M.; Occhiello, E. Polymer Surfaces from Physics to Technology; Wiley: Chichester, England, 1994, p 166.
9. Clark, D. T.; Feast, W. J. J Macromol Sci Revs Macromol Chem 1975, C-12, 191.
10. Beamson, G.; Brigg, D. High Resolution XPS of Organic Polymers; Wiley: New York, 1992.